



Synthesis, spectral and thermal characterization of metal complexes derived from 4-((3,5-dibromo-2-hydroxy benzylidene) amino) benzene sulphonamide: *In-vitro* antimicrobial and anticancer activities

J. Anandakumaran, M. L. Sundararajan, G. Ramasamy and T. Jeyakumar*

Chemistry section, Faculty of Engineering and Technology, Annamalai University, Annamalai Nagar, 608002, India

ABSTRACT

In this present work, we report the synthesis and characterization (IR, ¹H NMR, ¹³C NMR, molar conductance, mass spectra, UV-Visible, thermal analysis, EPR, and Powder XRD) of Schiff base namely 4-((3, 5-dibromo-2-hydroxy benzylidene) amino) benzene sulphonamide and its metal complexes. The bidentate coordination of ligand through phenolic oxygen and imine nitrogen (-CH=N-) was confirmed using spectral data. With the help of TGA, number of water molecules in coordination sphere of complexes was predicted. The geometry of complexes was proposed using EPR spectra. In-vitro antimicrobial activity of compounds L, L-Cd, L-Cu, and L-Zn was evolved with five bacterial and two fungal strains, In-vitro anticancer activity toward HeLa (human cervical cancer cell) was carried out for compounds L, L-Cd, L-Cu, L-Zn and L-Mn, wherein, L-Cd shows potent inhibitory effect against HeLa cell line.

Key words: Synthesis, 3, 5-dibromo salicylaldehyde, Schiff base, Sulphonamide, Metal complexes, Biological activities

INTRODUCTION

In the development of coordination chemistry, metal complexes of Schiff bases occupy a main role [1]. Transition metal complexes of Schiff base compounds are used as growth inhibiting agents for most of bacteria and fungi also they are widely used as potential therapeutics [2], they are useful in health and skin care [3]. Moreover, transition metal ion Schiff base complexes can be applied, particularly in agrochemical and pharmaceutical industries [4].

More attention on Schiff bases containing halogen atoms and their metal complexes is due to their antimicrobial properties [5]. The wide investigations of Schiff bases derived from substituted salicylaldehydes and various amines and their metal complexes is due to their enormous biological applications [6-9]. The ligands possess O and N donor atoms show broad biological activity and have special interest on bonding to metal ions [10, 11]. The enhanced biological activities like antitumor, antibacterial and antifungal activities are observed in salicylaldehyde derivatives, with one or more halo-atoms in the aromatic ring [12, 13]. The synthesis of metal sulphonamide compounds has received much attention due to their effective chemotherapeutic nature when employed for the prevention and cure of bacterial infections in humans. Considerable attention has been paid by many researchers over the synthesis of sulphonamide derivatives, because of their ability to coordinate with metal atoms in different ways [14-18]. Furthermore, the aromatic amino group of sulphonamide derivatives are versatile one, since it can act as coordinating site as well as reactive site for chemical modification. In view of previous findings, here we synthesized 4-((3, 5-dibromo-2-hydroxy benzylidene) amino) benzene sulphonamide (L) derived from 3, 5 – dibromo salicylaldehyde and sulphanilamide, and also its transition (II) metal complexes. The structures of entire new compounds were confirmed with the results of spectral and elemental analyses. Moreover we reported the antimicrobial screening as well as anticancer activity against HeLa cell line for selected compounds.

EXPERIMENTAL SECTION

2.1 Materials

All chemicals used in the present work *viz.*, sulfanilamide, 3, 5-dibromo salicylaldehyde, $\text{CuCl}_2 \cdot 2\text{H}_2\text{O}$, $\text{Ni}(\text{CH}_3\text{COO})_2 \cdot 4\text{H}_2\text{O}$ and $\text{Cd}(\text{CH}_3\text{COO})_2 \cdot 2\text{H}_2\text{O}$, $\text{ZnCl}_2 \cdot 6\text{H}_2\text{O}$, $\text{CoNO}_3 \cdot 6\text{H}_2\text{O}$ and $\text{Mn}(\text{NO}_3)_2 \cdot 2\text{H}_2\text{O}$ were of analar grade (Sigma - Aldrich). Ethanol and methanol were used after distillation. The remaining reagents were procured from commercial sources.

2.2 Instrumentation

Carbon, hydrogen and nitrogen (C, H & N) analysis were performed by Thermofinnigan elemental analyzer. UV-Visible spectra of the ligand and metal complexes were recorded in the range of 200–800 nm using Shimadzu UV-1650 spectrophotometer. Infrared spectra were recorded on Avatar 330 FT-IR, in the range of 4000–400 cm^{-1} using KBr pellets. ^1H and ^{13}C NMR spectra (at room temperature) were recorded on a Bruker Magnet System in 400 MHz/54 mm (Ultra Shield Plus) using DMSO as a solvent and TMS as internal standard. Thermal analysis (TG/DTA) was carried out using, SDT Q 600 thermal analyzer in the temperature range 20–1000 °C, in nitrogen atmosphere at a heating rate of 20 °C min^{-1} . The mass spectra were recorded by using JEOL GCMATE II GC-MS. X-ray diffraction spectra of the Schiff base and its metal complexes were carried out with powdered compounds using XPERT-PRO diffractometer system at 25 °C in Cu anode material [K-Alpha1 (Å) 1.54060, K-Alpha2 (Å) 1.54443 K-Beta (Å) 1.39225] and the generator settings as 30 mA, 40 kV. EPR spectrum of Schiff base copper complex was carried out using JEOL Model JES FA200 EPR instrument with X- Band frequency: 8.75 - 9.65 GHz, Sensitivity: 7×10^9 spins/0.1mT, resolution: 2.35 μT , variable temperature in the range -170 to +200 °C. Melting point was measured using Gallenkamp melting point apparatus. Molar conductance of the entire compounds was determined in DMSO at room temperature using a CMD 750 WPA conductivity meter.

3. Synthesis of 4-((3, 5-dibromo-2-hydroxy benzylidene) amino) benzene sulphonamide (L)

The Schiff base ligand was synthesized by refluxing 3, 5-dibromosalicylaldehyde (0.02 mol) with sulfanilamide (0.02 mol) in methanol (50 mL) for 6 h. After the solvent has been removed by evaporation in vacuum, the resultant product was filtered, dried, washed several times with hot methanol and recrystallized. The recrystallized product was dried under vacuum over anhydrous CaCl_2 . Red colour solid, yield 90 %. m.p. 220–222 °C. Anal. Calc. for $\text{C}_{13}\text{H}_{10}\text{N}_2\text{SO}_3\text{Br}_2$ (%): C (35.97), H (2.32), N (6.45); found: C (35.93), H (2.23), N (6.41). MW: 434.09. κ ($\Omega^{-1} \text{cm}^2 \text{mol}^{-1}$): 4.42. IR (KBr, cm^{-1}): 3317 $\nu_{\text{asym}}(\text{NH}_2)$, 3240 $\nu_{\text{sym}}(\text{NH}_2)$, 1625 $\nu(\text{C}=\text{N})$, 1155 $\nu_{\text{asym}}(\text{SO}_2)$, 1230 $\nu(\text{C}-\text{OH})$. ^1H NMR (DMSO - d_6 , 400MHz) δ ppm: 14.150 (OH, phenolic, 1H), 9.039 (HC=N, 1H), 7.998–7.635 (aromatic protons, 6H), 7.454 (NH_2 , 2H). ^{13}C NMR (DMSO - d_6 , 400MHz) δ : 164.18 (HC=N, 1C), 156.94 – 122.06 (Aromatic carbons, 12C). MS (GC), m/z (%): M^+ 433.78.

3.1 Synthesis of complexes

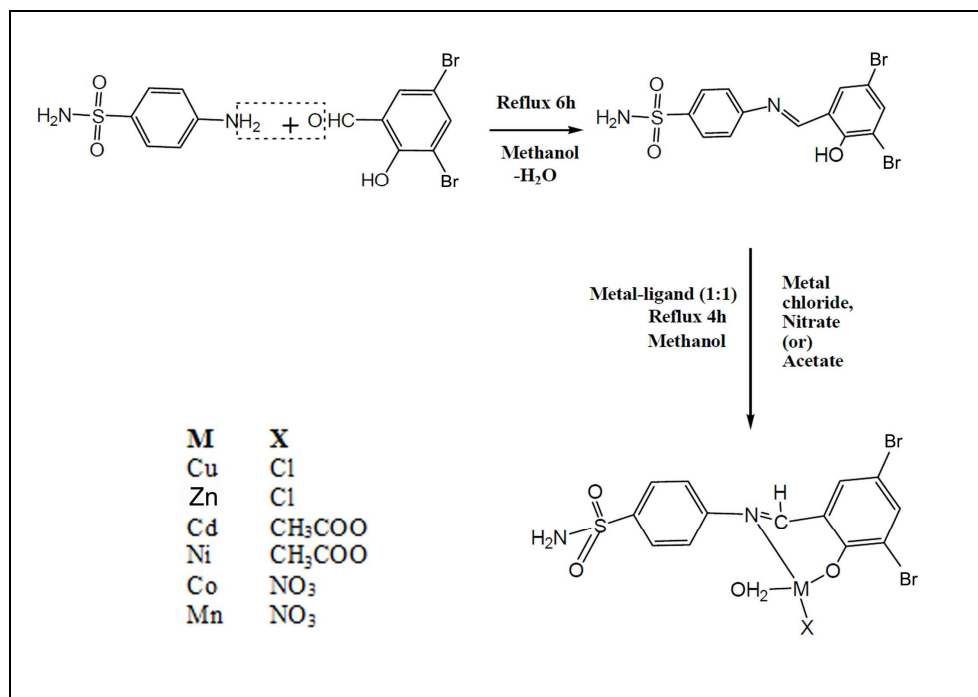
A methanolic solution of ligand (0.002 mol) was mixed with metal chloride or nitrate or acetate (0.002 mol) keeping metal ligand ratio 1:1. The mixture was refluxed for 4 h. The solid product precipitated on cooling was collected by filtration and washed with hot methanol until the washings become colourless. The product was dried in vacuum over CaCl_2 . All metal complexes are coloured and stable to air and moisture.

4-((3, 5-dibromo-2-hydroxy benzylidene) amino) benzene sulphonamide. Cd (L-Cd): Red colour solid. Yield 45 %. m.p. 180–182 °C. Anal. Calc. for $\text{C}_{15}\text{H}_{16}\text{N}_2\text{SO}_7\text{Br}_2\text{Cd}$ (%): C (28.12), H (2.51), N (4.37); found: C (28.63), H (2.60), N (4.58). MW: 640.566. κ ($\Omega^{-1} \text{cm}^2 \text{mol}^{-1}$): 2.24. IR (KBr, cm^{-1}): 3323 $\nu_{\text{asym}}(\text{NH}_2)$, 3230 $\nu_{\text{sym}}(\text{NH}_2)$, 1632 $\nu(\text{C}=\text{N})$, 1157 $\nu_{\text{asym}}(\text{SO}_2)$, 1237 $\nu(\text{C}-\text{OH})$, 833 $\nu(\text{H}_2\text{O}, \text{coord})$ 553 $\nu(\text{M}-\text{O})$, 456 $\nu(\text{M}-\text{N})$. ^1H NMR (DMSO - d_6 , 400MHz) δ ppm: 8.839 (HC=N, 1H), 8.007–7.635 (aromatic protons, 6H), 7.456 (NH_2 , 2H), 1.910 (CH_3 , 1H). ^{13}C NMR (DMSO - d_6 , 400MHz) δ : 199.01 (COO, 1C), 160.81 (HC=N, 1C), 156.49 – 121.96 (Aromatic carbons, 12C), 20.14 (CH_3 , 1C) MS (GC), m/z (%): M^+ : 640.566

4-((3, 5-dibromo-2-hydroxy benzylidene) amino) benzene sulphonamide. Ni (L-Ni): Green colour solid. Yield 30%. m.p. >300 °C. Anal. Calc. for $\text{C}_{15}\text{H}_{16}\text{N}_2\text{SO}_7\text{Br}_2\text{Ni}$ (%): C (30.70), H (2.74), N (4.77); found: C (30.76), H (2.81), N (4.82). MW: 586.846 κ ($\Omega^{-1} \text{cm}^2 \text{mol}^{-1}$): 2.16. IR (KBr, cm^{-1}): 3300 $\nu_{\text{asym}}(\text{NH}_2)$, 3200 $\nu_{\text{sym}}(\text{NH}_2)$, 1635 $\nu(\text{C}=\text{N})$, 1152 $\nu_{\text{asym}}(\text{SO}_2)$, 1203 $\nu(\text{C}-\text{OH})$, 831 $\nu(\text{H}_2\text{O}, \text{coord})$ 557 $\nu(\text{M}-\text{O})$, 455 $\nu(\text{M}-\text{N})$. MS (GC), m/z (%): M^+ : 586.830

4-((3, 5-dibromo-2-hydroxy benzylidene) amino) benzene sulphonamide. Cu (L-Cu): Brown colour solid. Yield 40%. m.p. 200–202 °C. Anal. Calc. for $\text{C}_{13}\text{H}_{13}\text{N}_2\text{SO}_5\text{Br}_2\text{ClCu}$ (%): C (27.48), H (2.30), N (4.93); found: C (27.62), H (2.39), N (5.02). MW: 568.105 κ ($\Omega^{-1} \text{cm}^2 \text{mol}^{-1}$): 2.82. IR (KBr, cm^{-1}): 3315 $\nu_{\text{asym}}(\text{NH}_2)$, 3225 $\nu_{\text{sym}}(\text{NH}_2)$,

1636v(C=N), 1155v_{asym}(SO₂), 1236v(C-OH), 842v(H₂O, coord) 551v(M-O), 470v(M-N).MS(GC), m/z (%): M⁺: 568.105



Scheme -1- 4 -((3, 5-dibromo-2-hydroxy benzylidene) amino) benzene sulphonamide Metal complexes

4-((3, 5-dibromo-2-hydroxy benzylidene) amino) benzene sulphonamide. Zn (L-Zn): Orange colour solid. Yield 75 %. m.p. >300 °C. Anal. Calc. for C₁₃H₁₃N₂SO₅Br₂ClZn (%): C (27.39), H (2.29), N (4.91); found: C (27.46), H (2.31), N (4.89). MW: 569.955. K (Ω⁻¹ cm²mol⁻¹): 2.24. IR (KBr, cm⁻¹): 3322v_{asym}(NH₂), 3232v_{sym}(NH₂), 1630v(C=N), 1152v_{asym}(SO₂), 1205v(C-OH), 827v(H₂O, coord) 547v(M-O), 455v(M-N). ¹H NMR (DMSO - d₆, 400MHz) δ ppm: 8.919 (HC=N, 1H), 7.985-7.634(aromatic protons, 6H), 7.455 (NH₂, 2H). ¹³C NMR (DMSO - d₆, 400MHz) δ : 160.18(HC=N, 1C), 156.69 – 121.69 (Aromatic carbons, 12C)MS(GC), m/z (%): M⁺569.955

4-((3, 5-dibromo-2-hydroxy benzylidene) amino) benzene sulphonamide. Co (L-Co): Brown colour solid. Yield 90%. m.p. 168-170 °C. Anal. Calc. for C₁₃H₁₃N₃SO₈Br₂Co (%): C (26.46), H (2.21), N (7.12); found: C (26.70), H (2.36), N (7.30). MW: 590.048. K (Ω⁻¹ cm²mol⁻¹): 2.32. IR (KBr, cm⁻¹): 3315v_{asym}(NH₂), 3255v_{sym}(NH₂), 1635v(C=N), 1149v_{asym}(SO₂), 1205v(C-OH), 827v(H₂O, coord), 561v(M-O), 463 v(M-N).MS(GC), m/z (%): M⁺590.536

4-((3, 5-dibromo-2-hydroxy benzylidene) amino) benzene sulphonamide. Mn(L-Mn): Blackish brown colour solid. Yield 80%. m.p. >300°C. Anal. Calc. for C₁₃H₁₃N₃SO₈Br₂Mn (%): C (26.64), H (2.23), N (7.16); found: C (26.84), H (2.41), N (7.30). MW: 586.048 K (Ω⁻¹ cm²mol⁻¹): 2.46 IR (KBr, cm⁻¹): 3319v_{asym}(NH₂), 3250v_{sym}(NH₂), 1639v(C=N), 1155v_{asym}(SO₂), 1236 v(C-OH), 831v(H₂O, coord), 551v(M-O), 470v(M-N).MS(GC), m/z (%): M⁺586.047.

3.2 Biological activities

The antibacterial activity of the synthesized compounds was determined against five bacterial strains *viz.*, *Escherichia coli* (*E. coli*), *Staphylococcus aureus* (*S. aureus*), *Enterococcus faecalis* (*E. faecalis*), *P.aurogenes* and *K. pneumonia*. Ampicillin was used as reference antibacterial agent. *In vitro* antibacterial activity was determined by agar well diffusion method [19] as described in our previous work [20].

Antifungal activity of the ligand (L) and its metal complexes was screened against two fungi *viz.*, *Candidaalbicans* (*C. albicans*) and *A. niger* according to the guidelines in the National Committee for Clinical Laboratory Standards (NCCLS) approved standard document M27-A2 [21]. Streptomycin was used as reference antifungal agent. MIC of the synthesized compounds were determined by serial dilution tube method as mentioned in our previous work [20]. For both the activities the concentration of compound was maintained at 400µg.

3.3 Anticancer activity:

The anticancer activity was performed at Tata Memorial Centre Advanced for Treatment, Research and Education in Cancer (ACTREC), Khar, Navi Mumbai – 410210, (HeLa cell line) by SRB assay. The principle behind SRB assay is, under acidic conditions, a bright pink aminoxanthine dye SRB binds dye to basic amino acid residues in TCA (Trichloro acetic acid) fixed cells to provide a sensitive index of cellular protein content that is linear over a cell density range of visible at least two order of magnitude [22, 23].

The cell count of trypsinized monolayer cell culture was adjusted to $0.5-1.0 \times 10^5$ cells/ml using 10% new born sheep serum medium. To each well of the 96 well micro titre plate, 0.1ml of the diluted cell suspension (approximately 10,000 cells) was added. After 24 hours, when a partial monolayer was formed, the supernatant was flicked off, washed once and 100 μ l of different test compound concentrations were added to the cells in micro titre plates. Following compounds addition, plates were incubated at 37 °C for 72 hours in 5% CO₂, 95% air and 100% relative humidity. Every 24 hours microscopic examination was carried out and results were recorded. After 72 hours, 25 μ l of 50% trichloroacetic acid was added to the wells gently such that it forms a thin layer over the test compounds to form overall concentration 10 % and incubated for 60 min. at 4 °C. To remove traces of medium, sample and serum the plates were flicked and washed five times with tap water and then air dried. The air-dried plates were strained with 100 μ l SRB and kept for 30 min. at room temperature. After straining, the unbound dye was removed by rapidly washing four times with 1 % acetic acid and then air dried. To solubilize the dye, 100 μ l of 10 mM Tris base was then added and the plates were shaken vigorously for 5 min. The absorbance was measured using microplate reader at a wavelength of 540 nm. The percentage growth inhibition was calculated using following formula,

$$\% \text{ cell inhibition} = 100 - \left\{ \frac{(A_t - A_b)}{(A_r - A_b)} \right\} \times 100$$

Where, A_t = Absorbance value of test compound,
 A_b = Absorbance value of blank,
 A_r = Absorbance value of reference.

RESULTS AND DISCUSSION

The condensation of sulfanilamide with 3,5-dibromosalicylaldehyde in 1:1 molar ratio yields Schiff base which on further reaction with metal salts *viz* CuCl₂.2H₂O, ZnCl₂.6H₂O, Ni(CH₃COO)₂.4H₂O, Cd(CH₃COO)₂.2H₂O, Co(NO₃)₂.2H₂O and Mn(NO₃)₂.2H₂O in metal ligand ratio 1:1 yielded the corresponding complexes, (L-M) which are given in (scheme 1)

4.1 Physical Properties and UV-Vis spectra

The 1:1 metal ligand ratio of the complexes was confirmed by elemental analysis. The observed molar conductance of the complexes in DMSO solution (1×10^{-3} M) are non-electrolytes, since it does not have any counter ion.

The UV-Vis spectra of entire compounds were recorded in DMSO at room temperature. The spectrum of the ligand (L) exhibits two bands at 297 and 442 nm attributed to $\pi-\pi^*$ and $n-\pi^*$ transition within the ligand. In the spectra of complexes, $\pi-\pi^*$ band remains unaltered, whereas $n-\pi^*$ band is blue shifted between 290 and 390 nm region due to the polarization within the $>C=N$ chromophore which caused by the formation of covalent metal-nitrogen bond [29]. The above observations confirm the charge transfer from ligand to metal charge transition (LMCT) [25].

4.2 IR spectra

The structures of newly synthesized ligand and its complexes were characterized by FT-IR technique and the resulting spectra are given in Fig. 1. The ligand used in this investigation is neutral which contains two coordination sites. The peak appeared at 1624 cm^{-1} in the spectrum of ligand due to azomethine group ν (C=N) is shifted to higher frequency ($6-15 \text{ cm}^{-1}$) on metal coordination. This observation helped us to prove the coordination of azomethine nitrogen with metal [26, 27]. The shifting is due to the donation of electron from the lone pair of azomethine nitrogen to the empty d-orbital of the transition metal atom. Except ligand all the metal complexes shows broad band at 3454 (L-Cd), 3464 (L-Ni), 3450 (L-Co), 3460 (L-Mn), 3441 (L-Zn), and 3439 cm^{-1} (L-Cu) may be due to ν (OH) of water. The NH₂ stretching vibration band observed at 3317 and 3240 cm^{-1} in ligand, does not show much deviation in the spectra of complexes. This indicates the non-involvement of NH₂ group in complexation.

Similarly, the absorption bands appeared at 1325 and 1155 cm^{-1} due to asymmetric and symmetric stretching vibration respectively of SO₂ group in ligand, appeared with more or less at the same position in metal complexes suggests the non-involvement of SO₂ group in complex formation [28]. In spectra of complexes, the IR band ν (H₂O) appeared at $802-850 \text{ cm}^{-1}$ indicating the binding of water molecules to the metal ions [29]. Moreover L-Cd and L-Ni complexes showed the coordination of acetate group by the appearance of new bands due to $\nu_{\text{asym}}(\text{COO})$ and

$\nu_{\text{sym}}(\text{coo})$ at 1572 – 1573 cm^{-1} and 1415-1442 cm^{-1} respectively [30]. L-Co and L-Mn shows two new bands at 1381 – 1382 cm^{-1} and 1205 cm^{-1} due to the coordination of nitrate group in the coordination complex [31]. A new band appeared at lower frequency region 524 – 553 cm^{-1} and 455 – 470 cm^{-1} is due to (M-O) and (M-N) coordination respectively. A sharp band in ligand spectrum appeared at 1230 cm^{-1} [32] due to (C-OH) stretching vibration of phenol is shifted to higher or lower frequency in complexes (L – Cu: 1236 cm^{-1} , L-Cd: 1237 cm^{-1} , L-Ni: 1203 cm^{-1} , L-Co: 1205 cm^{-1} , L-Mn: 1207 cm^{-1} , L-Zn: 1265 cm^{-1}) indicates the coordination of phenolic oxygen with metal atoms [33].

Table 1: Powder XRD, hkl calculation for L-Cu complex

Position (2 θ)	d-spacing (Å)	Relative intensity (%)	D ²	1000/D ²	(1000/D ²)/ Common factor	hkl
16.1849	5.4765	100.00	29.99205	33.34217	1.7127	1 1 0
21.9359	4.052	41.63	16.4187	60.90615	3.128589	1 1 1
25.0189	3.5592	21.80	12.6679	78.93965	4.054923	2 0 0
28.8424	3.0955	26.60	9.58212	104.361	5.360753	2 1 0
31.7087	2.8219	31.13	7.96312	125.5789	6.45066	2 1 1
33.9616	2.6397	25.96	6.968016	143.5129	7.37188	-----
44.7707	2.0243	18.22	4.09779	244.034	12.73538	3 2 0
45.3437	2	11.25	4	250	12.84184	3 0 2
57.3528	1.6065	13.06	2.580842	387.4704	19.90334	3 3 1
68.5687	1.3886	17.86	1.92821	518.6157	26.63993	4 3 1

Table 2 –Mass loss (%) & Temperature range of TGA curve for the complexes

Complex	Steps			
		First	Second	Third
L- Cd	Temp. θ° C	20-330	331-900	1000
	% Loss	30.0	49.9	20.1
L – Ni	Temp. θ° C	20-370	371-900	1000
	% Loss	32.0	55.0	13.0
L – Cu	Temp. θ° C	20-360	361-900	1000
	% Loss	34.0	52.5	13.5
L – Zn	Temp. θ° C	20-370	371-900	1000
	% Loss	34.0	52.0	14.0
L – Co	Temp. θ° C	20-370	371-900	1000
	% Loss	33.1	54.74	12.9
L – Mn	Temp. θ° C	20-370	371-900	1000
	% Loss	31.0	56.0	13.0

Table 3 Antimicrobial activity of Ligand & metal complexes (zone of inhibitors in mm)

Microbial Strains	L	L-Zn	L--Cu	L-Cd	Positive control
<i>E.coli</i>	15	15	30	11	31
<i>S.aureus</i>	10	11	11	12	28
<i>E.feacalis</i>	16	20	29	25	31
<i>P.aurogenes</i>	12	9	11	-	30
<i>K.pneumonia</i>	14	20	11	12	31
<i>C.albicans</i>	15	21	28	23	25
<i>A.niger</i>	15	22	29	19	24

Table. 4 Parameters Calculated from cell line

Human Cervical Cancer Cell Line HeLa																
% Control Growth																
Drug Concentrations ($\mu\text{g/ml}$)																
	Experiment 1				Experiment 2				Experiment 3				Average Values			
	10	20	40	80	10	20	40	80	10	20	40	80	10	20	40	80
L	65.8	37.7	-12.0	-58.2	62.1	40.4	-8.3	-61.1	44.0	30.0	-18.6	-74.5	57.3	36.0	-13.0	-64.6
L-cd	34.7	-11.4	-47.3	-65.6	60.5	24.6	-27.6	-63.4	26.2	-30.4	-77.1	-84.6	40.5	-5.7	-50.7	-71.2
L-Mn	97.0	75.3	35.7	-19.8	117.3	93.0	55.1	-7.8	103.3	77.5	34.2	-23.7	105.9	82.0	41.7	-17.1
L-zn	112.3	120.9	98.8	39.4	135.3	134.3	117.4	52.7	111.3	124.0	107.8	42.2	119.6	126.4	108.0	44.8
L-cu	103.6	96.8	38.3	-0.9	130.6	113.8	57.6	10.5	103.1	102.2	40.9	6.7	112.4	104.3	45.6	5.5

4.3 ¹H and ¹³C NMR spectra

NMR is a tool to identify the exact number of protons as well as carbon in the structure of compounds. ¹H NMR spectra of ligand (L) and its diamagnetic complexes (L-Zn and L-Cd) were recorded in DMSO using tetramethylsilane (TMS) as internal standard. A representative spectrum is given in Fig. 2. ¹H NMR spectrum of ligand (L) shows a signal at δ 14.150 ppm with integral value 1 is attributed to phenolic proton [34]. The multiple signals observed between δ 7.635 and 7.998 ppm are due to aromatic protons. The signal appeared at δ 9.039 ppm is assigned to imine proton (–HC=N–) with an integral value one. The signal at δ 7.454 ppm with an integral value two is assigned to –NH₂ protons [35]. The signal appeared for imine proton in free ligand at δ 9.010 ppm is shifted to

up field in L-Cd and L-Zn complexes indicates the metal nitrogen coordination. A signal, which was observed at δ 14.150 ppm in ligand spectrum has been completely disappeared in L-Cd and L-Zn complex spectra, confirms the involvement of phenolic oxygen in coordination. Meanwhile a new signal appeared at δ 1.910 ppm corresponding to three proton integrals attributed to coordination of acetate group with metal. Taken together, ^1H NMR spectral observations support the bidentate nature of ligand.

In ^{13}C NMR spectra of ligand, signals between δ 122.06 and 156.94 ppm are due to aromatic carbons. The signal due to imine carbon ($-\text{HC}=\text{N}-$) at δ 164.18 ppm [36] is shifted to up field in the spectra of L-Cd and L-Zn complexes at δ 160.81 ppm and δ 160.18 ppm respectively, indicating the involvement of azomethine in complex formation. The ^{13}C NMR spectrum of complex L-Zn shows no progressive change in aromatic carbon compared with free ligand. However, in L-Cd complex, two signals appeared at δ 199.01 ppm and δ 20.14 ppm, confirms the involvement of acetate group in coordination. A representative spectrum is shown in Fig. 2 &3.

Table. 4 a Parameters Calculated from cell line

HeLa	Parameters Calculated from cell line		
	LC50	TGI	GI50*
L	68.6	39.8	10.9
L-Cd	56.97	22.5	<10
L-Mn	>80	68.2	39.3
L-Zn	>80	>80	80.4
L-Cu	>80	79.6	48.2

LC₅₀ - Concentration of drug causing 50 % cell kill

GI₅₀ - Concentration of drug causing 50 % inhibition of cell growth

TGI - Concentration of drug causing total inhibition of cell growth

FGI₅₀ - Values of < 10 μg is considered to demonstrate potent activity in of pure case compounds

4.4 X-ray powder diffraction

Powder X-ray diffractometry of the samples was performed without any further treatment such as hand grinding. In addition, the experiments were performed in specially fabricated sample holders (of a modified polymer) to protect them from the ambient moisture. Among powder X-ray diffraction analysis of all the compounds, (Fig. 4) only ligand, Cu and Mn complexes display defined sharp peaks indicating their crystalline nature, whereas, the broadening of peaks in all other complexes may reveals their amorphous nature. Amorphous materials do not depict any significant peak in diffraction pattern [37, 38]. Crystalline nature of the complexes was indicated by comparing the XRD pattern of the ligand and complexes. The $h^2 + k^2 + l^2$ values are determined for all the complexes by unit cell calculations. The result reveals that all the complexes are tetragonal geometry due to the presence of forbidden number 7 [39]. A representative calculation is given in Table 1. The structure of complexes could not be determined due to the unavailability of single crystals. Each complex has specific d values, which can be used in its characterization [40, 41]. The crystallite sizes (t) are calculated using the Scherrer equation [42].

$$t = \kappa\lambda/\beta (\text{Cos}\theta) \dots \dots \dots (1)$$

Where κ is Scherrer constant = 0.9, λ is the wavelength of X-ray, θ is the peak position measured in radian, and β is the integral breadth of reflections (in radians 2θ) located at 2θ . The calculated average crystallite size for ligand: 28.44 nm and its metal complexes: 28.22 nm (L-Co), 28.68 nm (L-Cd), 28.19 nm (L-Cu), 28.28 nm (L-Zn), 28.39 nm (L-Mn) and 28.41 nm (L-Ni).

4.5 Thermogravimetric Analysis

Thermogravimetric analysis of transition metal complexes was one of the useful techniques to identify the availability of water molecules in complexes as well as to know the stability of the metal complexes. In the present study, heating rates were controlled at $20^\circ\text{C min}^{-1}$ under nitrogen atmosphere and weight loss was measured up to 1000°C (Fig. 5). The weight loss percentage at various stages are summarized in Table 2.

In Cd complex, mass losses were occurred in three stages. The first stage at $20 - 330^\circ\text{C}$, corresponds to loss of SO_2 , NH_2 , C_6H_4 , and one lattice and one coordinated water molecule (found : 30.0 %, cal: 29.9 %). The second stage decomposition with mass loss of 41.9 % (cal: 41.8 %) at $331 - 900^\circ\text{C}$ was attributed to the remaining organic molecule. Final decomposition of 20.1 % (cal: 20.04 %) mass loss was due to CdO.

For Ni complex, the first step is in the temperature range of $20 - 370^\circ\text{C}$, with the mass loss of 32.0 % (calc: 32.74 %) may account for SO_2 , NH_2 , and C_6H_4 and two (one lattice and one coordinated) water molecules. The second step occurs within the temperature range $371 - 900^\circ\text{C}$ which corresponds to the removal of organic molecule with a mass loss of 55.0 % (calc: 54.53 %). In the final step metal oxide was leaving as residue (found: 13.0 %, calc: 12.72 %)

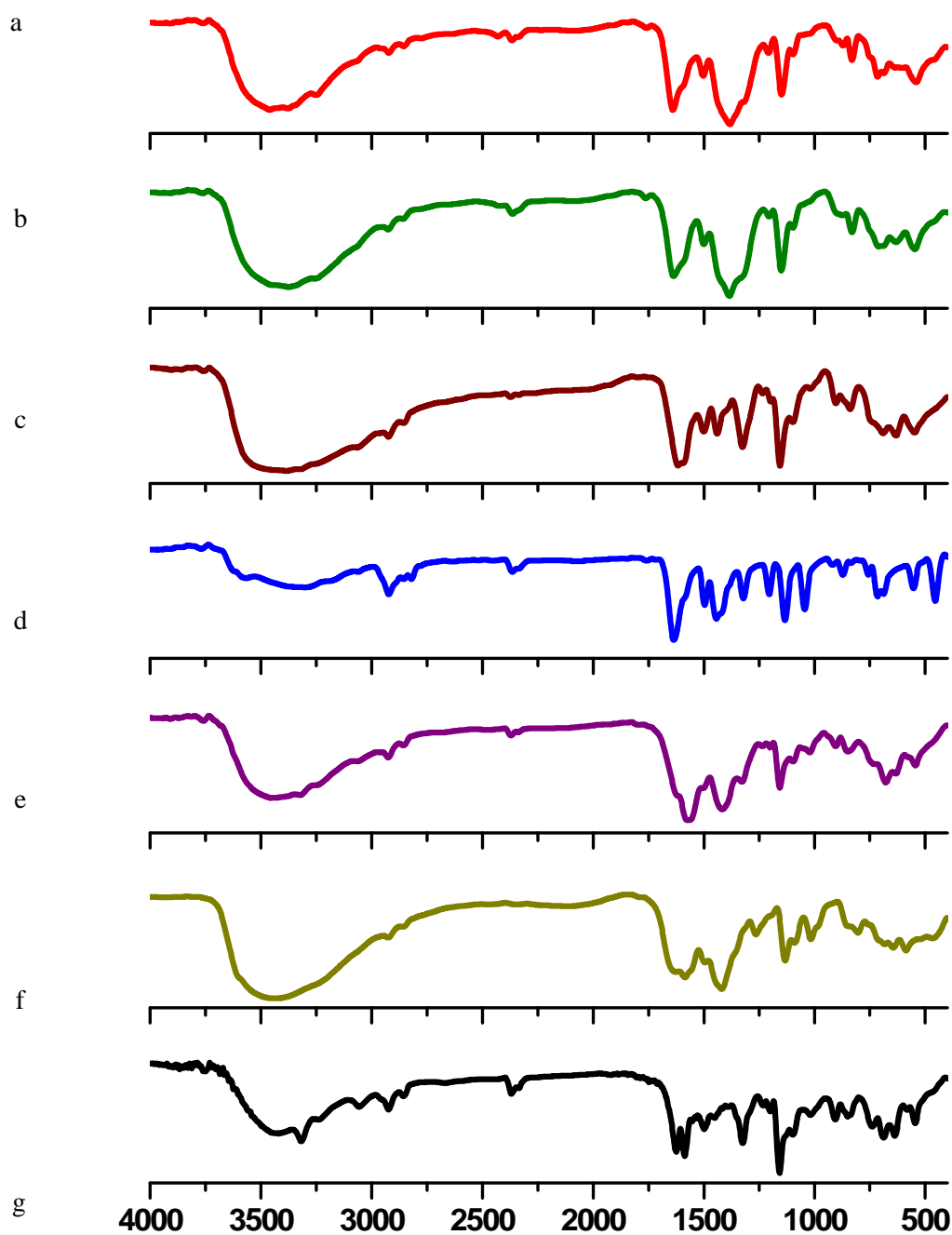


Fig : 1 IR spectra of Ligand & metal complexes, (a) L-Zn (b)L -Mn (c) L-Co (d) L-Cu (e) L-Ni (f) L-Cd (g) Ligand

The thermogram of Cu shows first step of decomposition in temperature range of 20 to 360 °C with mass loss of 34 % (calc: 34.8%) due to SO₂, NH₂, C₆H₄ and two water molecules. Both lattice as well as co-ordinated water molecules was decomposed within this temperature range. The remaining organic moiety has been decomposed from the molecule at 361 – 900 °C (mass loss, found 52.5 % calc: 52.17 %). Last step was the removal of residue metal oxide with a mass loss of 13.5 % (calc: 14.0%).

The first decomposition step in Zn complex at temperature range between 20 and 370 °C is due to the removal of SO₂, NH₂, C₆H₄ and two water molecules (one lattice and one co-ordinated water molecule) with mass loss found 34.0 % (calc: 33.71 %). The second step (371–900 °C) indicates the decomposition of C₆H₃Br₂ (found 52.0 %, calc: 52.10 %). Metal oxide is the stable residue at 1000 °C (found 14.0 %; calc: 13.9 %).

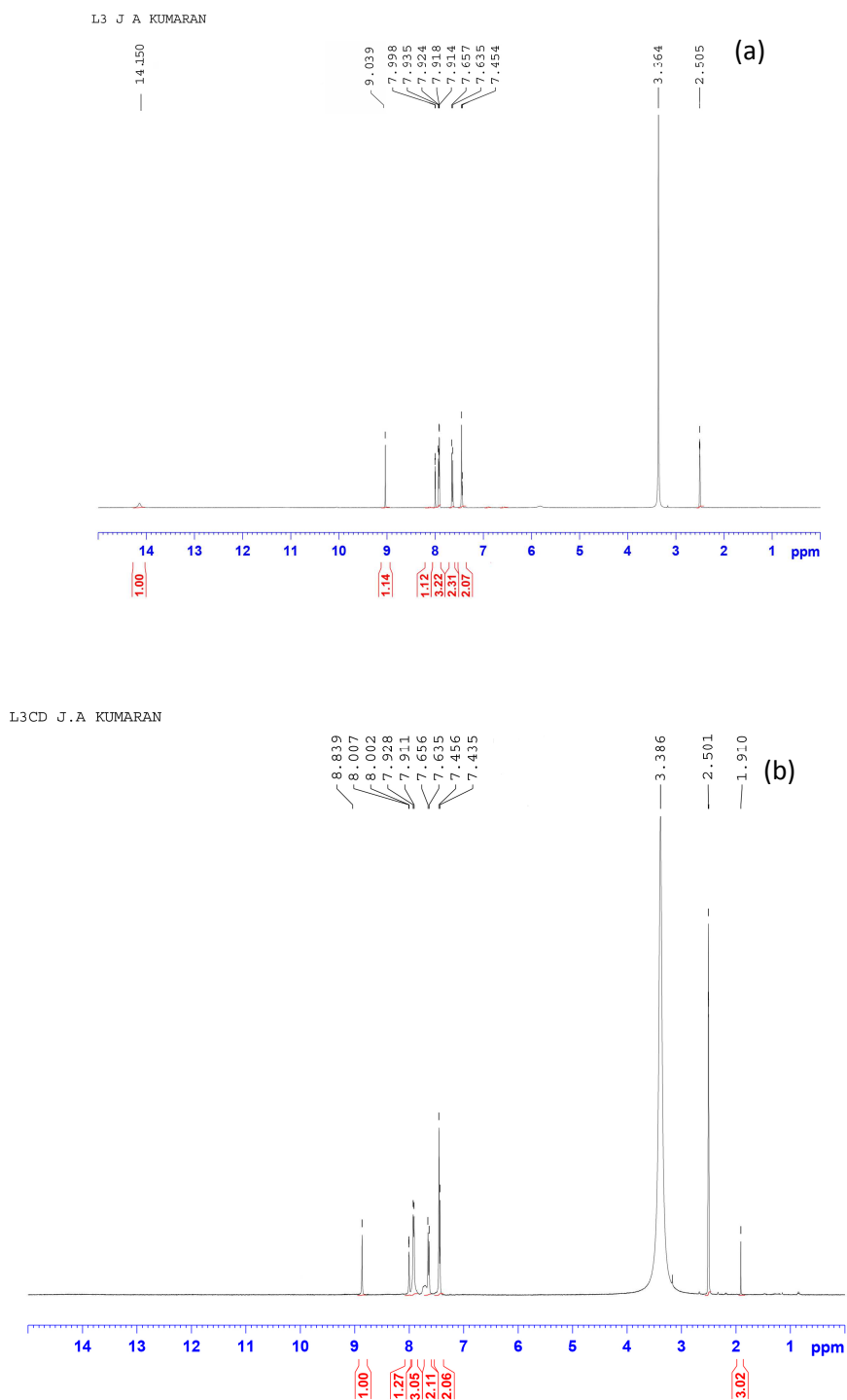


Fig. 2 – ^1H NMR spectra of ligand & metal complex (a) Ligand (b) L – Cd

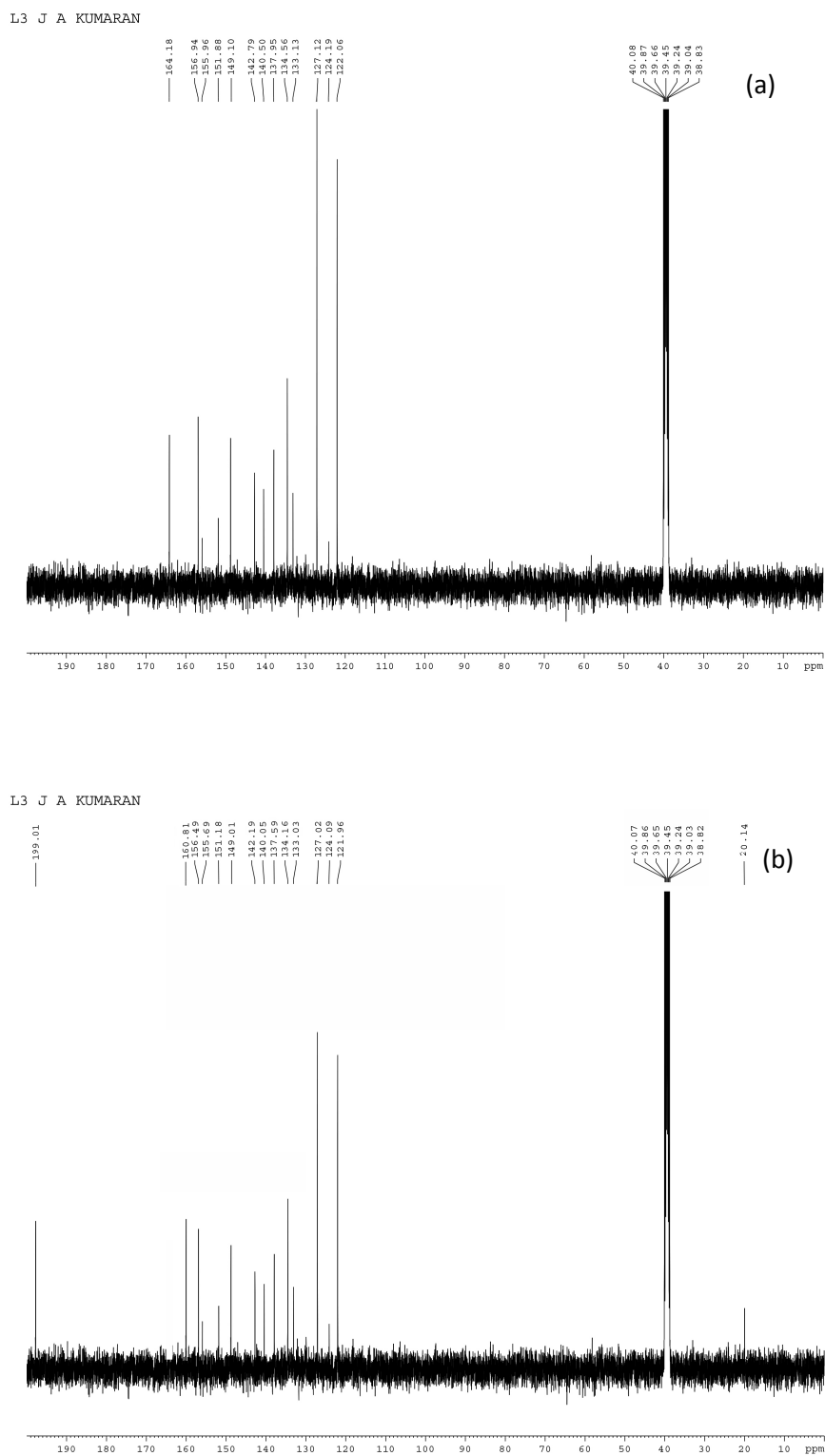
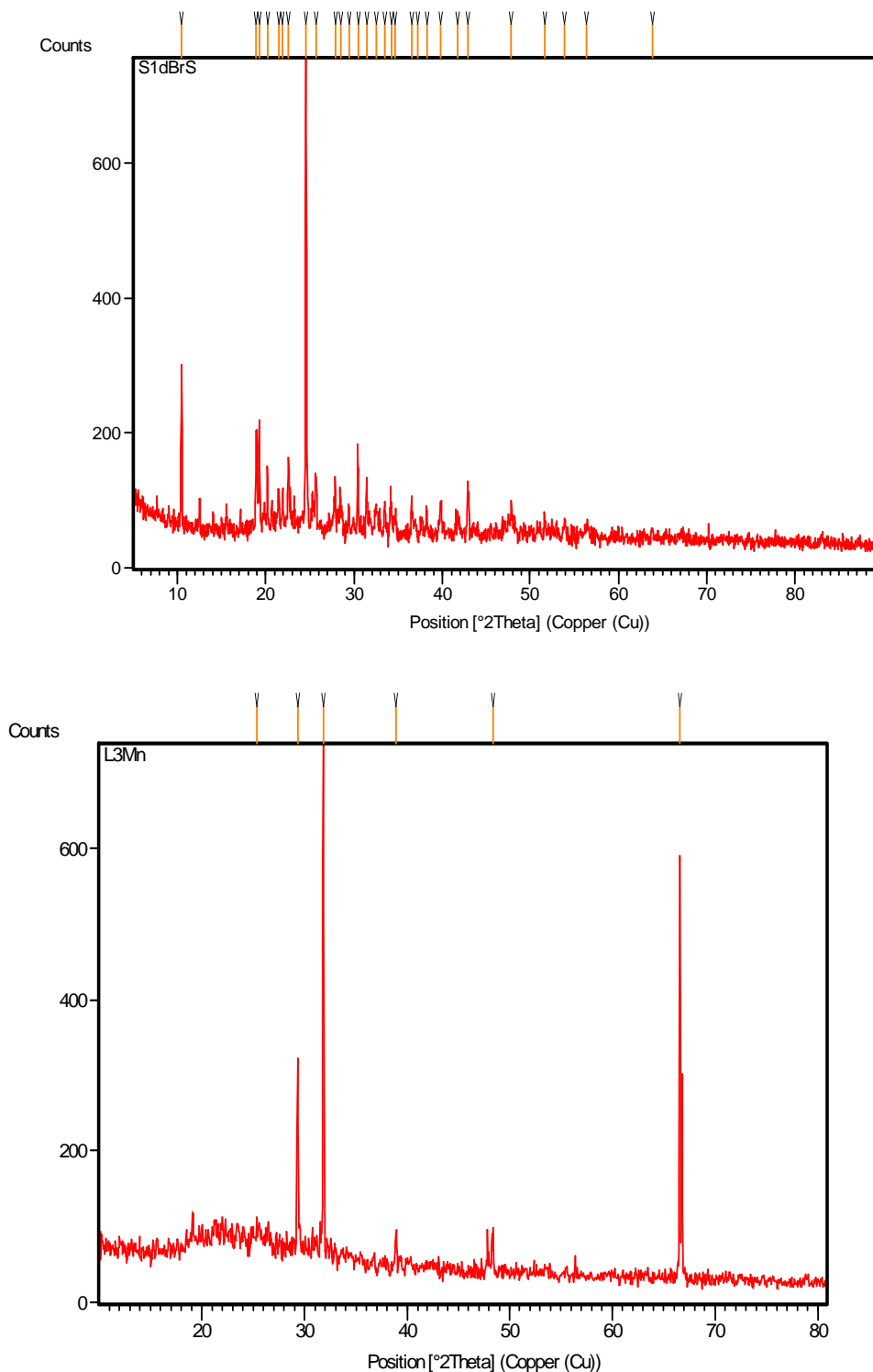


Fig. 3. ¹³CNMR spectra of ligand and complex (a) Ligand (b) L-Cd



**Fig. 4 Powder XRD of Ligand & metal complexes
L- Mn**

In Co complex, the decomposition is characterized by steps at 20 -370 °C, 371- 900 °C and >900 °C corresponds to the removal of lattice and co-ordinated water molecules, SO₂, NH₂, and C₆H₄ (found 33.10 %, calc: 32.56 %), remaining organic molecule (found 54.0 %, calc: 54.74 %) and metal oxide (found 12.90 %, calc: 12.69 %).

Similarly in Mn complex, the first step of decomposition was due to SO₂, NH₂, C₆H₄ and two water molecules (temp range 20 – 370 °C) with mass loss of 31.0 % (calc : 32.78 %). The subsequent steps (371 – 900 °C) correspond to the removal of organic part of the ligand (found 56.0 %, calc: 55.13 %) leaving metal oxide as residue.

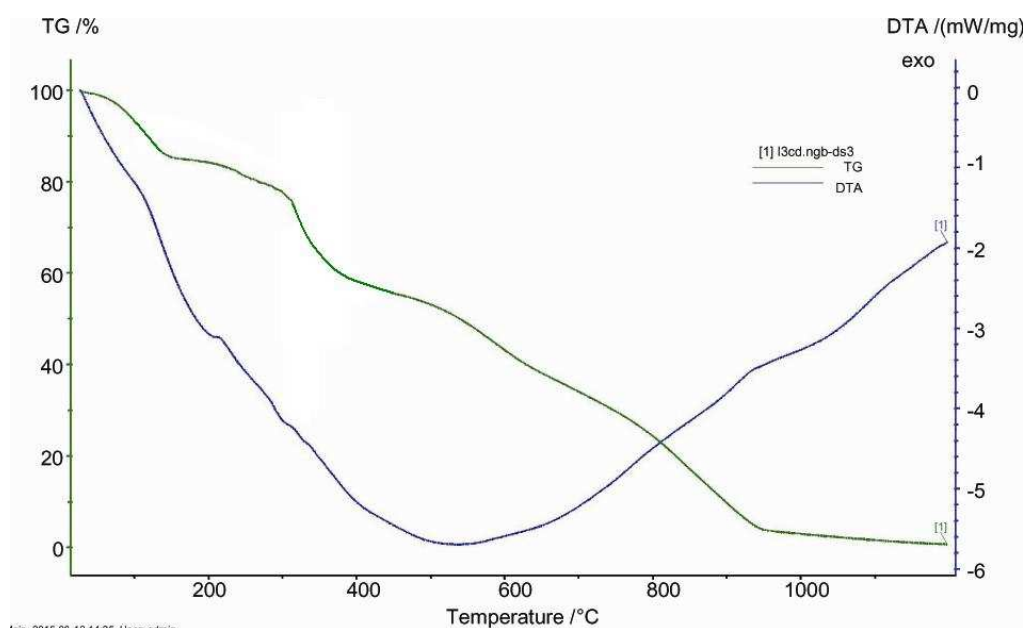


Fig. 5. Thermogram of metal complexes L- Cd

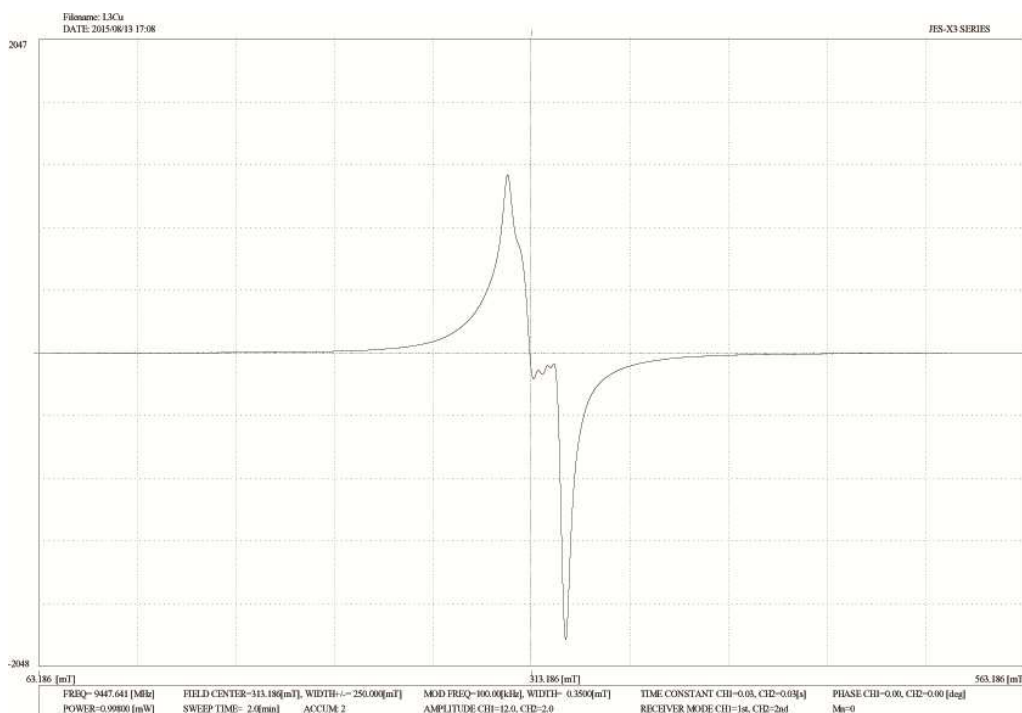


Fig. 6 EPR of L – Cu complex

4.6 EPR

EPR studies of Copper (II) complex (Fig. 6) was carried out on the X-band at 9.4 GHz under the magnetic field strength 3000 G. The spectrum was recorded in DMSO at room temperature. The spin Hamiltonian parameters for the copper complex are calculated from the spectra. The explicit formulae for Cu (II) with a single electron in dx^2-y^2 are

$$A_x = A_y = [-\kappa + 2/7 + 11/14(g_{x,y} - g_e)] P \quad \rightarrow 1$$

$$A_z = [-\kappa - 4/7 + (g_z - g_e)] P \quad \rightarrow 2$$

With P = energy unit for dipolar interaction $\sim 0.035 \text{ cm}^{-1}$ and $\kappa = 0.23$. The trend $g_{\parallel} > g_{\perp} > 2.0024$ [$(A_{\parallel} = 184 \times 10^{-4} \text{ cm}^{-1}) > A_{\perp} = 94 \times 10^{-4} \text{ cm}^{-1}$; $g_{\parallel} = 2.3413 > g_{\perp} = 2.0674$] indicated that the copper the one unpaired electron is localized in dx^2-y^2 orbital of the Cu (II) ion and the spectral figures are characteristic for the axial symmetry tetragonal

geometry. [43] For copper complex $g_{\parallel} = 2.34$ which is in between 2.3 - 2.4, thus shows mixed copper-nitrogen and copper-oxygen bonds in these chelate [44, 45]. The parameter G , determined as $G = (g_{\parallel} - 2)/(g_{\perp} - 2)$, The Cu(II) complex reported in this paper gave the “ G ” values which are greater than 4 [i.e 5.1] indicating the exchange interaction is absent in solid complex [46]. The bonding parameters of this complex can be calculated with the help of optical spectra of the complex.[47]. The molecular orbital coefficients in-plane π – bonding (β^2) and in-plane σ – bonding (α^2) were calculated using following expressions [48]

$$\alpha^2 = (A_{\parallel} / 0.036) + (g_{\parallel} - 2.0023) + 3/7 (g_{\perp} - 2.0023) + 0.004 \quad \rightarrow 3$$

$$\beta^2 = (g_{\parallel} - 2.0023) E / -8\lambda\alpha^2 \quad \rightarrow 4$$

The spin-orbit coupling constant, λ value (-534 cm^{-1}) calculated using the relations, $g_{av} = 1/3[g_{\parallel} + 2g_{\perp}]$ and $g_{av} = 2(1 - 2\lambda / 10Dq)$, is less than the free Cu (II) ion (-832 cm^{-1}) which also supports covalent character [49]. If the value of $\alpha^2 = 0.5$, it indicates complete covalent bonding, while the value of $\alpha^2 = 1.0$ suggests complete ionic bonding. The observed value of α^2 (0.65) of the complex is less than unity, which indicates that the complex has some covalent character in the ligand environment. [50]

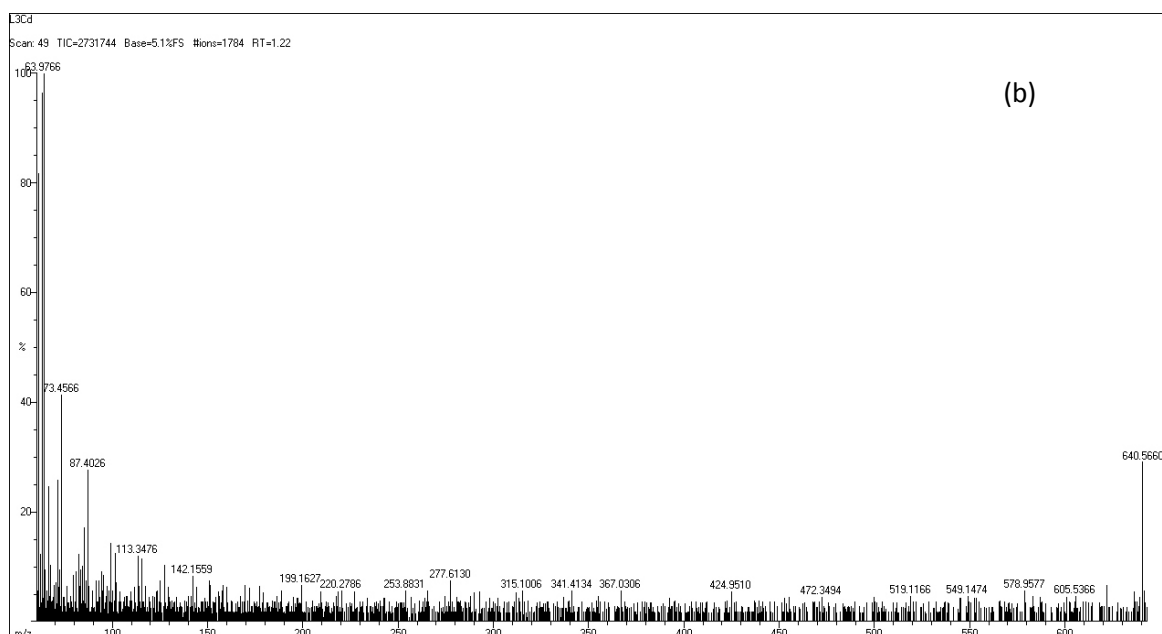
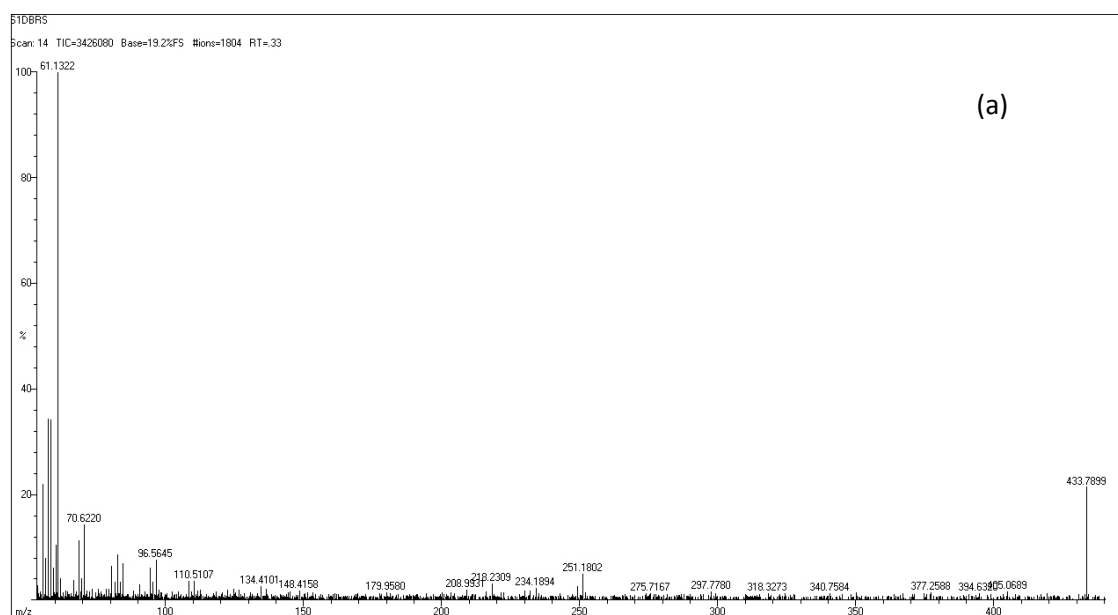


Fig 7 GC Mass spectra of ligand and complex(a) Ligand (b) L-Cd

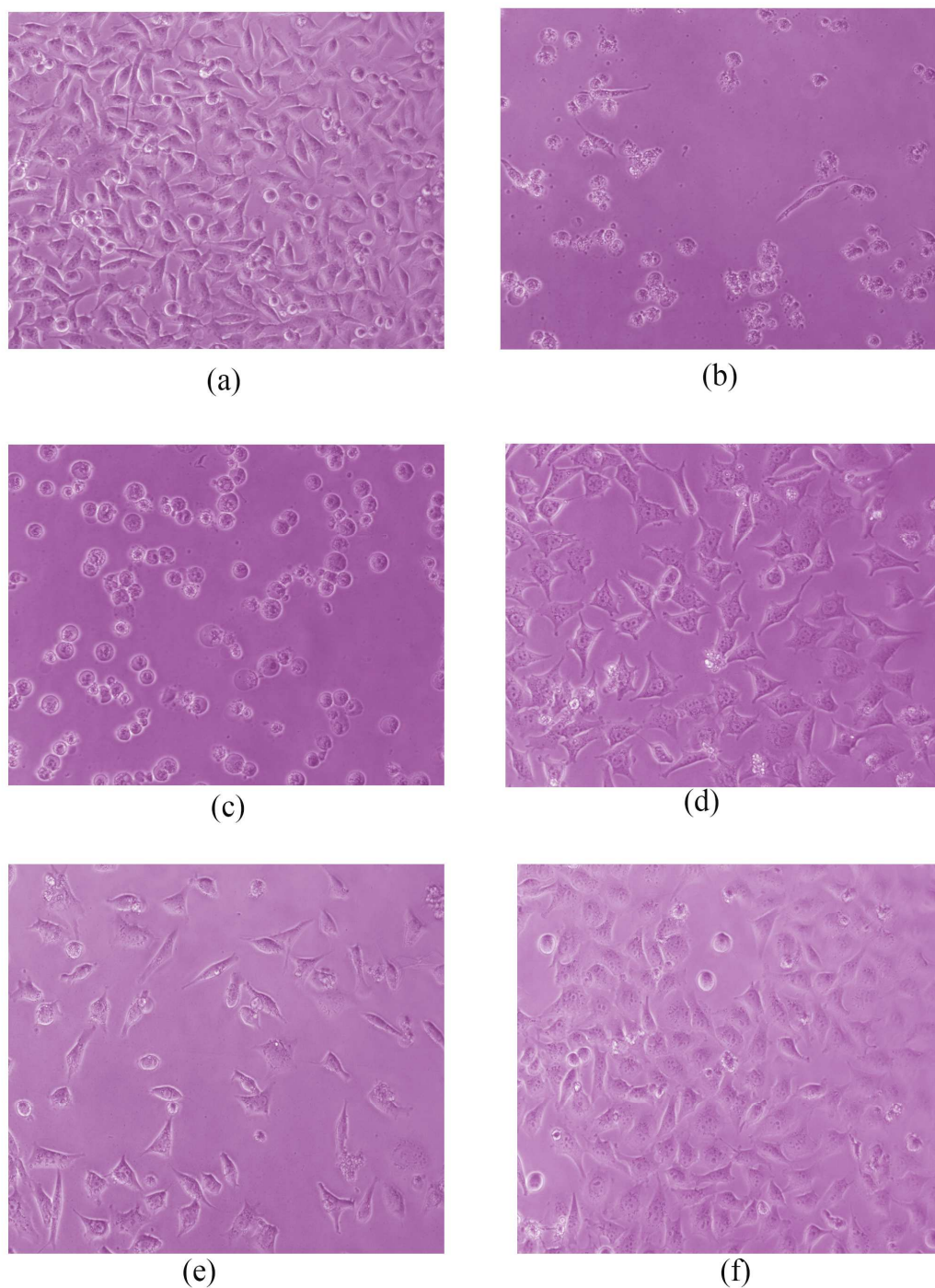


Fig. 8 Anticancer activity: Images of Ligand & metal complexes (a) Reference (b) ligand (c) L – Cd (d) L – Cu (e) L–Mn (f) L - Zn

4.7 Mass spectra

The mass spectra of the ligand and its transition metal complexes were recorded at ambient temperature. The observed molecular ion peaks in the mass spectra of the ligand and its metal complexes have been used to confirm the proposed formula mass (Scheme 1). A representative electron impact mass spectrum is shown in Fig. 7.

Mass spectrum of the ligand shows peak at m/z 433.789 is corresponding to molecular ion M. The ligand has fragmented up to 61 mass number. The mass spectra of complexes L-Cd, L-Ni, L-Cu, L-Zn, L-Co and L-Mn show a prominent peak at 640.566, 586.83, 568.105, 569.955, 590.538 and 586.047 respectively, which are consistent with the molecular mass of the respective metal complexes. The spectral data prove that the ratio between metal and ligand is 1:1 as described in Scheme 1.

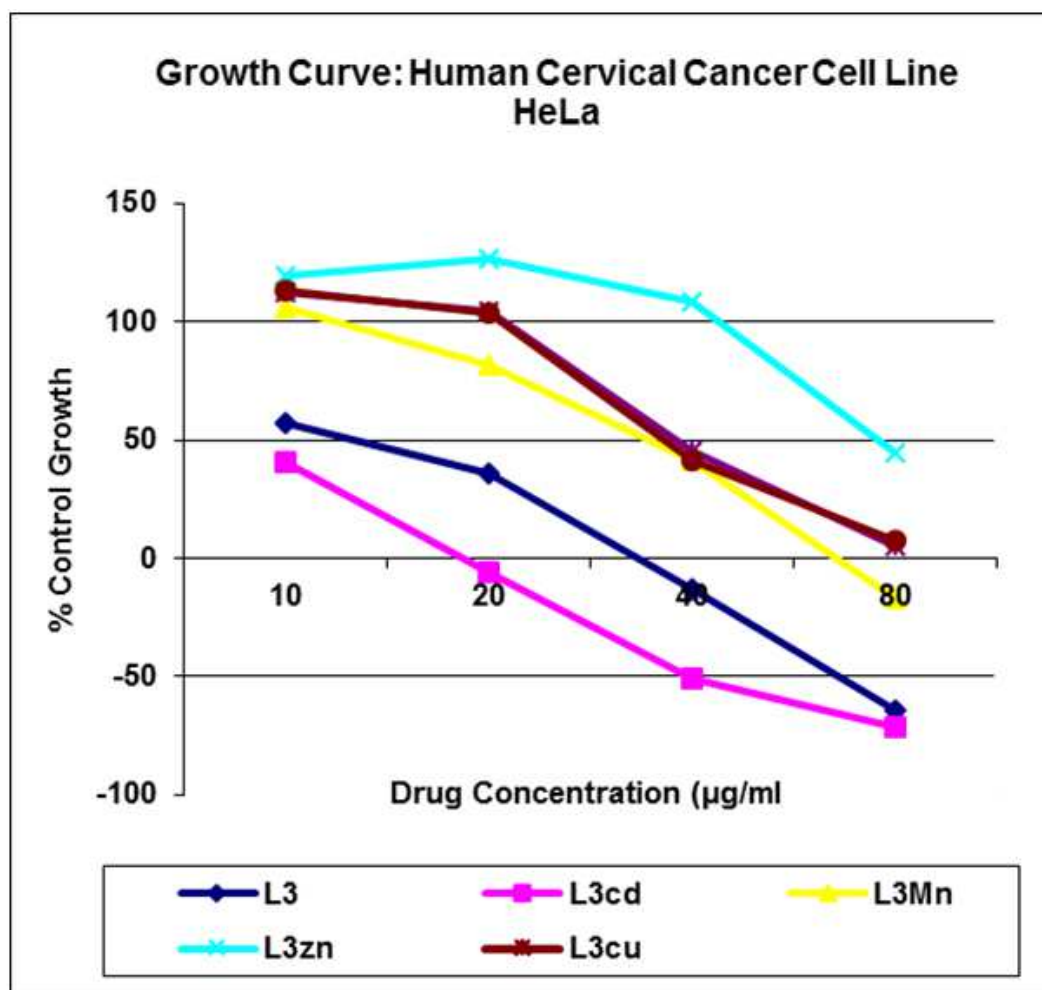


Fig. 9:- Anticancer activity: Growth curve

4.8 Antibacterial activity

The Schiff base and its L-Cu, L-Zn and L-Cd complexes were examined for their *in vitro* antibacterial activity against five human pathogenic bacteria (*E. coli*, *S. aureus*, *E. faecalis*, *P. aurogenes* and *K. pneumonia*) by well diffusion method using streptomycin as reference. The reference drug streptomycin is also tested for its antibacterial activity at the same concentration under the conditions similar to that of the test compounds concentration. By measuring the size of inhibition diameter, the susceptibility of bacterial strain towards the compounds is judged. The inhibition zone of bacteria in all compounds is given in Table 3. The minimum inhibition concentration (MIC) values of the compounds and reference against the respective bacterial strains were ranging between 20-150 µg /ml and 6-12.5 µg /ml, respectively. The obtained results suggest that the metal complexes are more active than ligand and less active than the reference against all the bacteria tested.

Among the compounds tested, highest activity was found for L-Cu complex towards the bacterial strains, *E. coli*, and *E. faecalis*. However, L-Cd and L-Zn, (MIC: 20-60µg/ml) show moderate activity against bacterial strains. The tested complexes L-Cu, L-Cd, L-Zn, possess high inhibitory power over the bacterial strain *E. faecalis*, herein the zone of inhibitions are 29, 25 and 20 mm respectively. More activity exhibited in metal complexes than the ligand is due to its chelation, which reduces the polarity of metal ion in complexes and thus favoring its permeation through lipid layer of microorganisms [51].

4.9 Antifungal activity

The compounds, which were used for antibacterial analysis, were used to test their antifungal activity against *candida albicans*, and *A. niger* by well diffusion method. The growth inhibition zone of compounds against microorganisms is summarized in Table 3. The MIC values of the compounds and reference *amphotericin B* (AMB) against the respective fungal strains were ranging between 20-100 µg / ml 0.03-16 µg / ml, respectively. The experimental results were compared with the reference at the same concentration of the test compounds. According to the zone of inhibition, we conclude that all the three complexes show good inhibition activity towards the fungal

strain *candida albicans*, and *A. niger*. Among the three complexes tested, in L-Cu, we found higher zone of inhibition than the positive control used. From the results, it has been observed that the fungal activity depends upon the nature of metal ion.

4.10 Anticancer activity

We investigated the *in-vitro* anticancer effects of newly synthesized ligand (L) and its metal complexes (L-Cd, L-Cu, L-Mn and L-Zn) on malignant cell line (human cervical HeLa cell) growth using sulforhodamine B protein (SRB) assay protocols [52] in order to assess their anticancer effects. Since the solubility of the tested compounds in aqueous medium was poor, they were dissolved in DMSO. By using SRB protocols, each drug was tested at four dose levels (10, 20 40, 80 µg/ml). Appropriate positive control (reference) Adriamycin (ADR) was used in each experiment and each experiment was repeated thrice. The results, in terms of GI₅₀ TGI and LC₅₀ are summarised in Table 4.

Using ADR as reference molecule, the obtained data revealed that the 50% inhibition concentration values (GI₅₀) are moderate to good activity ranging from <10 to 80.4 µg/ml. In particular, L-Cd potently inhibited HeLa at <10 µg/ml like ADR, whereas the remaining compounds moderately inhibited HeLa with GI₅₀ value range of 10.9 to 80.4 µg/ml. In general, inhibitory effects of the compounds are in order L-Cd > L > L-Mn > L-Cu > L-Zn. Corresponding images are shown in Fig. 8.

Meanwhile, concentration of drug that produces total inhibition of the cells (TGI) shows 22.5 and 39.8 µg/ml for compound L-Cd and L respectively, exhibited more potent. Moderate activity was found in L-Mn, and L-Cu, whereas no activity was found in L-Zn. Among four dose level of compounds, maximum inhibitory activity was found at 80 µg/ml (Fig. 9). Percentage control growth results of compound L and L-Cd are in line with reference ADR.

CONCLUSION

The present study reports the synthesis, spectral and thermal characterization of a ligand 4-((3, 5-dibromo -2-hydroxy benzylidene) amino) benzene sulphonamide and its transition metal complexes. Using IR and NMR spectra of compounds, we conclude that the ligand has been coordinated with metal atom as bidentate manner through phenolic oxygen and imine nitrogen. Thermograms of entire complexes prove the presence of one coordinated and one lattice water molecule. EPR result supports the tetragonal geometry in complexes. The results of *in-vitro* antimicrobial activities predict higher activity in complexes than in ligand. Finally the anticancer activity of L, L-Cd, L-Mn, L-Zn, and L-Cu were examined against HeLa cell line, and found good activity in L-Cd when compared with reference ADR. Thus the order of activity is L-Cd > L > L-Mn > L-Cu > L-Zn.

Acknowledgment

We would like to thank Dr. JyotiKode, Officer In-charge, Anti-cancer Drug Screening Facility, ACTREC, Navi Mumbai, to conduct *in vitro* anticancer testing of our compounds on one cell line (HeLa).

REFERENCES

- [1] KF Ansari; C Lal, *Eur. J. Chem.*, **2009**,44,2294-2299.
- [2] U Bohme; B Gunther, *Inorg. Chem. Commun.*, **2007**,10,482-484.
- [3] LC Felton; JH Brewer, *Science*, **1947**,105,409-410.
- [4] P Nobha; M Vieites; BS Parajon-Costa; EJ Baran; H Cerecetto; P Draper; M Gonzalez; OE Piro; EE Castellano; A Azqueta; AL Cerain; A Monge-Vega; D Gambino, *J. Inorg. Biochim.*, **2005**,99,443-451.
- [5] JE Toth; GB Grindey; WJ Ehlhardt; JT Ray; GB Boder; JR Bewley; KK Klingerman; SB Gates; SM Rinzel; RM Schultz; LC Weir; JF Worzalla, *J. Med. Chem.*, **1992**,40,1014-1018.
- [6] JC Medina; D Roche; B Shan; RM Learned; WP Frankmoelle; DL Clark,
- [7] *Bioorg. Med. Chem. Lett.*, **1999**,9,1843-1846.
- [8] H Yoshino; N Ueda; J Nijjima; H Sugumi; Y Kotake; N Koyanagi; K Yoshimatsu; M Asada; T Watanabe, *J. Med. Chem.*, **1992**,35,2496-2497.
- [9] T Owa; H Yoshino; T Okauchi; K Yoshimatsu; Y Ozawa; N Hata Sugi; T Nagasu; N Koyanagi; K Kitoh, *J. Med. Chem.*, **1999**,42,3789-3799.
- [10] NC Baenziger; AW Struss, *Inorg. Chem.*, **1976**,15,1807-1809.
- [11] DS Cook; MF Turner, *J. Chem. Soc., Perkin Trans.*, **1975**,2,1021-1025.
- [12] NC Baenziger; SL Modak; CL Fox Jr, *Acta Crystallogr. Sect. C*, **1983**,39,1620-1623.
- [13] CJ Brown; DS Cook; L Sengier, *Acta Crystallogr., Sect. C*, **1985**,41, 718-720.
- [14] LL Marques; G Manzoni de Oliveira; E Schulz Lang; RA Burrow, *Z. Naturforsch*, **2005**,60b,318-321.

- [15] E Schulz Lang; LL Marques; G Manzoni de Oliveira, *Z. Naturforsch.*, **2005**,60b,1264-1268.
- [16] LL Marques; G Manzoni de Oliveira; E Schulz Lang, *Z. Anorg. Allg. Chem.*, **2006**,632,2310.
- [17] E Schulz Lang; RA Burrow; LL Marques, *Acta Crystallogr., Sect. C*, **2003**,59,m95-96.
- [18] E Schulz Lang; LL Marques; RA Burrow, *Acta Crystallogr., Sect. E*, **2003**,59,m707-709.
- [19] LL Marques; E Schulz Lang; H Fenner; EE Castellano, *Z. Anorg. Allg. Chem.*, **2005**,631,745.
- [20] AU Rahman; MI Choudhary; WJ Thomsen, Bioassay techniques for drug development, Harwood Academic Publishers, Amsterdam, The Netherlands, **2001**,16.
- [21] ML Sundararajan; J Anandakumaran; T Jeyakumar; B Karpanai Selvan, *Spectrochim. Acta A*, **2014**,131,82-93.
- [22] National Committee for Clinical Laboratory Standards, Reference method for broth dilution antifungal susceptibility testing of yeasts, Approved Standard, 2nd edition, NCCLS Document M27- A2, NCCLS, Wayne, PA, USA **2002**.
- [23] P Skehan; R Storeng; D Scudiero; A Monks; J McMahon; D Vistica, *Proceedings of the American Association for Cancer Research*, **1989**,30, 612.
- [24] P Skehan; R Storeng; D Scudiero; A Monks; J McMahon; D Vistica, *J. National Cancer Institute.*, **1990**,82(13),1107-1112.
- [25] RW Masters, Animal cell culture, Cytotoxicity and viability assays, 3rd edition, **2000**,202-203.
- [26] FA Cotton; G Wilkinson, Advanced Inorganic Chemistry, Wiley Inter science, New York, Vol 5, **1988**,725-730.
- [27] C Saxena; RV Singh, *Synth. React. Inorg. Met-Org. Chem.*, **1992**,22,1061-1072.
- [28] RC Maurya; P Patel, *Spec. Lett.*, **1999**,32(2),213-236.
- [29] RC Maurya; P Sharma; D Sutradhar, *Synth. React. Inorg. Met-Org. Chem.*, **2003**,33,669-682.
- [30] RC Maurya; A Pandey; D Sutradhar, *Indian J. Chem.*, **2004**,43A,763.
- [31] CM Sharaby, *Spectrochim. Acta A*, **2007**,66,1271-1278.
- [32] HDS Yadav; SK Sengupta; SC Tripathi, *Inorg. Chim. Acta.*, **1987**,128,1-6.
- [33] RK Jain; AP Mishra, *current chem. Lett.*, **2012**,1,163-174.
- [34] ML Sundararajan; J Anandakumaran; T Jeyakumar, *Spectrochim. Acta A*, **2014**,125,104-123.
- [35] N Karabocek; S Karabocek; F Kormali, *Turk. J. Chem.*, **2007**,31,271-277.
- [36] RR Coombs; MK Ringer; JM Blacquiere; JC Smith; JS Neilsen; YS Uh; JP Gilbert; LJ Leger; H Zhang; AM Irving; SL Wheaton; CM Vogels; SA Westcott; AF DeckenBaerlocher, *Turk. J. Chem.*, **2008**,32,229-235.
- [37] NA Salih, *Met.Chem.*, **2005**,30,411-418.
- [38] A Chauhan; P Chauhan, *J. Anal. Bioanal. Tech.*, **2014**,5(5),1-5.
- [39] FG Vogt; GR Willams, *Am. Pharm. Rev.*, **2010**,13,58-65.
- [40] MR Karekal; MBH Mathada, *Turk. J. Chem.*, **2013**,37,775-795.
- [41] AD Khalaji; SM Rad; G Grivani; D Das, *J. Therm. Anal. Calorim.*, **2011**,103,747-751.
- [42] RS Joseyphus; CJ Dhanaraj; MS Nair, *Trans. Met. Chem.*, **2006**,31,699-702.
- [43] A Patterson, *A. Phys. Rev.*, **1939**,56,978-982.
- [44] RAA Ammar; AMA Alaghaz; AA Elhenawy, *J. Mol. Struct.*, **2014**,1067,94-103.
- [45] P Knopp; K Wiegardt; B Nuber; J Weiss; WS Sheldrick, *Inorg Chem.*, **1990**,29,363.
- [46] RK Ray; GR Kauffman, *Inorg. Chim. Acta.*, **1990**,173,207.
- [47] VSX Anthonisamy; R Murugesan, *Chem. Phys. Lett.*, **1998**,287,353-357.
- [48] TF Yen, Electron Spin Resonance of Metal Complexes, 1st Edition, Plenum Press, New York, **1969**,111-133.
- [49] N Raman; A Kulandaisamy; K Jeyasubramanian, *Ind. J. Chem.*, **2002**,41A,942-49.
- [50] BJ Hathway; DE Billing, *Coord. Chem.Rev.*, **1961**,5,143.
- [51] D Kevelson; RJ Niedman, *Chem. Phys.*, **1961**,35,149
- [52] G Kumar; D Kumar; CP Singh; A Kumar; VB Rana, *J. Serb. Chem. Soc.*, **2010**,75,629-637.
- [53] Terry Sharrer; HeLa Herself, *The Scientist*, 2006,20, 22.